IEICE TRANS. COMMUN., VOL.E103–B, NO.3 MARCH 2020

PAPER

Receiver Differential Code Bias Estimation under Disturbed Ionosphere Status Using Linear Planar Model Based Minimum Standard Deviation Searching Method with Bias Detection

Yan ZHANG[†], ***Student Member***, **Lei CHEN**[†a)], **Xiaomei TANG**[†], ***and*** **Gang OU**[†], ***Nonmembers***

SUMMARY Differential code biases (DCBs) are important parameters that must be estimated accurately for precise positioning and Satellite Based Augmentation Systems (SBAS) ionospheric related parameter generation. In this paper, in order to solve the performance degradation problem of the traditional minimum STD searching algorithm in disturbed ionosphere status and in geomagnetic low latitudes, we propose a linear planar based minimum STD searching algorithm. Firstly, we demonstrate the linear planar trend of the local vertical TEC and introduce the linear planar model based minimum standard variance searching method. Secondly, we validate the correctness of our proposed method through theoretical analysis and propose bias detection to avoid large estimation bias. At last, we show the performance of our proposed method under different geomagnetic latitudes, different seasons and different ionosphere status. The experimental results show that for the traditional minimum STD searching algorithm based on constant model, latitude difference is the key factor affecting the performance of DCB estimation. The DCB estimation performance in geomagnetic mid latitudes is the best, followed by the high latitudes and the worst is for the low latitudes. While the algorithm proposed in this paper can effectively solve the performance degradation problem of DCB estimation in geomagnetic low latitudes by using the linear planar model which is with a higher degree of freedom to model the local ionosphere characteristics and design dJ to screen the epochs. Through the analysis of the DCB estimation results of a large number of stations, it can be found that the probability of large estimation deviation of the traditional method will increase obviously under the disturb ionosphere conditions, but the algorithm we proposed can effectively control the amplitude of the maximum deviation and alleviate the probability of large estimation deviation in disturb ionosphere status.

key words: *differential code bias, linear planar fit, ionospheric disturbed status, estimation bias detection*

1. Introduction

Accurate estimation of Total Electron Content (TEC), which is one of the most important indicators to illustrate the spatial and temporal characters of ionosphere, is of great significance for the applications such as global ionosphere mapping, precise positioning, Satellite Based Augmentation Systems (SBAS) integrity ionospheric corrections calculation and establishment of SBAS ionospheric threat model. For accurate estimation of TEC, frequency-dependent satellite and receiver Differential Code Biases (DCBs) should be removed from GNSS measurements properly.

Manuscript received April 21, 2019.
Manuscript revised August 7, 2019.
Manuscript publicized September 20, 2019.

[†]The authors are with College of Electronic Science, National University of Defense Technology, Changsha, Hunan, P.R. China, 410073.
a) E-mail: Nightcat1025@163.com (Corresponding author)

DOI: 10.1587/transcom.2019EBP3092

Methods for DCBs estimation can be roughly divided into three groups. The first group is called equation solving method. It uses mathematical function to model the vertical TEC (vTEC) of different Ionospheric Pierce Points (IPPs). The coefficients of vTEC model and both the satellite and receiver DCBs are treated as unknowns that can be obtained from the solution of equations. This kind of method has been thoroughly researched and are the most widely used in DCB estimation with multiple stations' measurements. The first systematic method of deriving DCBs from GNSS observations was proposed by Lanyi and Roth in 1988 [1]. They model vTEC by a third order polynomial function of latitude and longitude and calculate the TEC and DCB simultaneously. Based on the same vTEC model, Coco [2] gave a research on the variability of the GPS L2-L1 satellite DCB. The results show that it remained quite stable with the variations less than 0.3 ns in 5 weeks. Paper mentioned above all used least square method in solving the observation equations. Kalman filtering technique were introduced by Sardon who model the state equations as random walk stochastic process [3]. Also other mathematical functions are used to model the ionosphere vTEC, such as spherical harmonics function [4], triangular series [5], spherical cap harmonic function model [6] and so on. Otsuka [7] proposed a mesh grid approach for DCB estimation which divides the ionosphere into small grids and the TEC at any point within a grid was assumed to be identical. Always several stations are needed to have a precise estimation result. What's more, the satellite and receiver DCBs are coupled in the observation equations and more constraints are required to separate them, i.e., the sum of the satellite DCBs is supposed to be zero. The second group is a kind of post-processing method which uses those already obtained vTEC results from IGS-IONEX files or other GIM products to extract the receiver DCB directly [8]. Compared to the first one, this kind of method can be applied for any ionospheric state, even in those disturbed days. However, it needs to use the vTEC map produced by the IGS data processing center which is an afterwards product and may not be available for any local receiver. The third group is called minimum standard deviation searching method. It was first proposed by Ma and Maruyama in 2003 [9]. By assuming the ionosphere is horizontally homogeneous, the estimated vTECs should be identical at an epoch for all the satellite IPPs over a certain elevation threshold when the receiver DCB is properly re-

moved. Thus, the receiver DCB is estimated by trying out a series of bias candidates and finding the one that gives a minimum standard deviation of vTECs. This kind of approach could provide high accurate DCB result with only one station observations and is vary computational efficient. However, because the ionosphere has a horizontal gradient and vertical structure, the vTECs of different satellite IPPs are not equal in actual cases. The degree of agreement between the mean value and the actual ionosphere characteristics is poor in disturb ionosphere status and geomagnetic low latitudes, and this may lead to a higher occurrence frequency of large biases.

In this paper, we mainly have a research on DCB estimation with single station observations in ionospheric disturbed status and geomagnetic low latitudes. Based on the method proposed by Ma (2003), we take the linear planar trend of local ionosphere into consideration and propose the linear planar model based minimum STD Searching method. Both theoretical analysis and experimental results show the effectiveness of our method. In Sect. 2, the GNSS dual-frequency observation model is introduced, and the minimum STD searching algorithm is introduced. In Sect. 3, we use the measured data from IGS to show that the linear planar model can realize a better description of the local ionosphere characteristics than the traditional constant model. Based on this, the minimum STD searching algorithm based on the linear planar model is designed, and its correctness is deduced theoretically. At the same time, based on the coincidence between the model hypothesis and the actual ionosphere observation, we design the bias detection indicator dJ to screen the epochs which will lead to better DCB estimation performance. In Sect. 4, some experiments are designed to display the performance of the proposed algorithm in different geomagnetic latitudes, different seasons and different ionosphere activities. Also the results are compared with the traditional methods to illustrate the effectiveness of the proposed algorithm. In Sect. 5, we summarize the main content of the article.

2. Extraction TEC Coefficients and DCBs from GNSS Observations

2.1 GNSS Observations

GNSS pseudorange and carrier phase can be modeled in the following formulas [10],

$$\begin{aligned}\rho^i_{k,j} &= r^i_j + c\left(\tau^i - \tau_j\right) + T^i_j + I^i_{k,j} + d^i_k + d_{k,j} + \varepsilon^i_{\rho,k,j}\\ \phi^i_{k,j} &= r^i_j + c\left(\tau^i - \tau_j\right) + T^i_j - I^i_{k,j} - b^i_{k,j} + N^i_{k,j} + \varepsilon^i_{\phi,k,j}\end{aligned} \tag{1}$$

where the subscripts $k = 1, 2$ refer to different frequency f_k and here we take the GPS L1 ($f_1 = 1575.42$ MHz) and L2 ($f_2 = 1227.60$ MHz) as an example. i and j refers to the satellite and station (receiver) respectively. r^i_j is the distance from the receiver j to the satellite i. τ^i and τ_j represent the satellite and receiver clock offsets. T^i_j is the time delay due to troposphere and is independent with frequency. $I^i_{k,j}$ stands for the ionosphere delay which have the same value but with opposite sign in pseudorange and carrier phase measurement. $\varepsilon^i_{\rho,k,j}$ and $\varepsilon^i_{\phi,k,j}$ stand for the terms due to noise and multipath. $N^i_{k,j}$ is the ambiguity in carrier phase measurement. $b^i_{k,j}$ is the phase advance of the satellite and receiver instrument bias. d^i_k and $d_{k,j}$ are the code delays for the satellite and receiver instrument biases. The absolute values of them are hard to obtain and we often define the difference between them, namely the satellite and receiver DCB. The model for GNSS observations also include other frequency related error sources such as antenna phase, yet since their influence on observations (generally in the order of centimeters) are far less than the DCBs, they are not spelled out in the equations.

The relationship between ionosphere delay and vTEC can be modeled as,

$$I^i_{k,j} = \frac{A}{cf_k^2}\frac{TEC^i_j}{E\left(\Theta^i_j\right)} \tag{2}$$

where $A = 40.3$, c is the speed of light in vacuum, $E\left(\Theta^i_j\right)$ is the elevation mapping function which makes the transition from slant to vertical direction [11].

$$E\left(\Theta^i_j\right) = \cos\left(\arcsin\left(\frac{R}{R+h_I}\sin\left(\alpha\Theta^i_j\right)\right)\right) \tag{3}$$

Where Θ^i_j is the satellite elevation angle, R is the earth radius of 6378.137 km, h_I is the ionospheric thin shell height of 506.7 km for CODE group, α is a constant with the value of 0.9782.

From the geometric-free linear combination of pseudorange (or the carrier phase) measurements of different frequency, we can obtain the residual terms which only consist of ionosphere delay and DCBs.

$$\begin{aligned}L^i_{\rho,j} &= \rho^i_{2,j} - \rho^i_{1,j} = \left(I^i_{2,j} - I^i_{1,j}\right) + D_j + D^i + \varepsilon^i_{\rho,j}\\ L^i_{\phi,j} &= \phi^i_{2,j} - \phi^i_{1,j} = -\left(I^i_{2,j} - I^i_{1,j}\right) - \left(b^i_{2,j} - b^i_{1,j}\right) + N^i_j + \varepsilon^i_{\phi,j}\end{aligned} \tag{4}$$

$\varepsilon^i_{\rho,j}$ is the combination of pseudorange noise in the f_1 and f_2 frequency, namely $\varepsilon^i_{\rho,j} = \varepsilon^i_{\rho,1,j} - \varepsilon^i_{\rho,2,j}$. The similar meanings are for $\varepsilon^i_{\varphi,j}$ and N^i_j. The D^i and D_j represent the satellite and receiver DCBs respectively.

$$\begin{aligned}D^i &= d^i_2 - d^i_1\\ D_j &= d_{2,j} - d_{1,j}\end{aligned} \tag{5}$$

$L^i_{\rho,j}$ is of no ambiguity but is noiser and more vulnerable to multipath. $L^i_{\varphi,j}$ has ambiguity but is more accurate. In this paper we use the carrier phase $L^i_{\varphi,j}$ to smooth the $L^i_{\rho,j}$ and get a high accurate geometric-free combination. At an epoch t, the smoothed geometric-free combination can be expressed

as [10],

$$\begin{aligned}\tilde{L}^i_j(t) &= \omega_t L^i_{\rho,j}(t)+(1-\omega_t)\left[\tilde{L}^i_j(t-1)+\left(L^i_{\phi,j}(t)-L^i_{\phi,j}(t-1)\right)\right] \\ &= \frac{A}{cE\left(\Theta^i_j\right)}\frac{f_1^2-f_2^2}{f_1^2 f_2^2}vTEC^i_j+\left(D_j+D^i\right)+\varepsilon^i_{\rho,\phi,j}\end{aligned} \tag{6}$$

where,

$$\omega_t = 1/T_{const} \tag{7}$$

T_{const} is the time constant.

2.2 Minimum STD Searching Method

In this subsection, we will give a brief description about the minimum STD searching method for single station DCB estimation.

We may have different vTEC results when different receiver DCB is applied in Eq. (6). Suppose that the vTEC result of a time epoch is $x^i(t)$ $(i = 1, 2, \ldots, M_t)$, where M_t is the number of visible satellites for a receiver with a certain elevation threshold constraint. The standard deviation of vTEC for a single epoch can be expressed as,

$$\sigma\left(t\left|D_j\right.\right) = \sqrt{\frac{1}{M_t}\sum_{i=1}^{M_t}\left(x^i(t)-\bar{x}(t)\right)^2\Big|_{D_j}} \tag{8}$$

where $\tilde{x}(t)$ is the mean value of $x^i(t)$.

The objective function can be constructed as the sum of single epoch STD which is shown in Eq. (8),

$$J = \frac{1}{N}\sum_{t=1}^{N}\sigma^2\left(t\left|D_j\right.\right) \tag{9}$$

where N is the epoch number. The estimated receiver DCB is the one that makes the minimization of J. The MS method does not need to solve the equations and thus is more computational convenient compared to the equation solving method. Also a more accurate result may be obtained when only one station's observations are available. Although need the satellite DCBs in advance, it is not that highly dependent on the ionosphere IONEX products compared to the post processing method because of the stability of satellite DCB. Xue [12] has found that over a long period, the standard deviations (STDs) for all satellite B1–B2 DCBs were within 0.3 ns (average: 0.19 ns) and for all satellite B1–B3 DCBs, the STDs were within 0.36 ns (average: 0.22 ns). And the similar results were for other satellite constellations. This approach is essentially based on the hypothesis that the vTEC results of different IPPs at a time epoch obey the zero-order constant model. However, the ionosphere variation is quite complicated and the horizontal and vertical homogenous properties are not always suitable assumptions. Especially in disturbed states and in geomagnetic low latitudes, the error caused by these assumptions cannot be ignored.

3. Single Station DCB Estimation Based on Linear Planar Model Method with Bias Detection

In the previous section, we introduce the minimum STD searching algorithm for single station DCB estimation. The basic assumption is that under a certain elevation constraint, a receiver has the same vTECs for different IPPs (regardless of observation noise). In this section, we will first analyze the measured data of IGS station and show that the linear planar (the first-order) hypothesis can achieve a better approximation of the local ionosphere characteristics compared with the constant (the zero-order) hypothesis. Secondly, we theoretically analyze the correctness of the linear planar based minimum STD searching algorithm, and design the bias detection indicator dJ which is originated from the degree of coincidence between the model hypothesis and the real ionosphere observations. This indicator dJ can also be used as a criterion for epoch selection to improve the performance of DCB estimation in the case of disturb ionosphere conditions and in geomagnetic low latitudes.

3.1 The Planar Trend of Local Ionosphere

In this subsection, we will choose three stations separately at geomagnetic high, mid and low latitudes to compare the ionosphere modeling performance of the traditional constant model and the proposed linear planar model under different ionosphere status. (Because the ionosphere activity is significantly affected by geomagnetic field activity, in this paper, we classify the position of the station from geomagnetic latitude rather than geographic latitude. It is generally considered that the range of geomagnetic low latitudes is from 20°S to 20°N, the range of geomagnetic mid latitudes is from 20°N to 50°N and from 20°S to 50 °S, and the range of geomagnetic high latitudes is from 50°N to 90°N and from 50 °S to 90 °S). Table 1 lists the names of our selected stations and their geographic and geomagnetic coordinates.

In Table 1, the positive and negative latitude value corresponds to the northern and southern latitude respectively. The positive and negative longitude value corresponds to the eastern and western longitude respectively. (In this paper, we use IGRF-11 [13] as a reference for the transformation between geographic coordinates and geomagnetic coordinates). It should be noted that the geomagnetic coordinates corresponding to a specific geographic coordinates will change with time, but the annual change is very small which is between −0.07° and 0.03°. Because we only use

Table 1 The coordinates of three stations located in high, mid, and low geomagnetic latitudes (in degree).

Station Name	Region	Geographic Lat	Geomagnetic Lat	Geographic Lon	Geomagnetic Lon
FAIR	High	64.97	65.39	-147.49	-98.10
GRAS	Mid	43.754	44.70	6.9205	88.64
BOGT	Low	4.64	14.90	-74.08	-2.41

the geomagnetic latitudes for classification, this change can be ignored in this paper.

3.1.1 Confirmation of the Ionosphere Status

When comparing the modeling performance of the constant model and the linear planar model under different ionosphere activity states, we first need to confirm the ionosphere status of the selected period. Ionosphere activity is affected by many factors, the most important of which are solar and geomagnetism, which can usually be indicated by the solar 10.7 cm radiation flux (f10.7), planetarische kennziffer (K_p) and disturbance storm time (D_{st}). However, these indices are the average results on a global scale, for a specific station (or in a local scale), we need to further confirm the ionosphere status. Following gives the selection and confirmation steps of the analysis period.

- Firstly, according to the K_p, D_{st} and f10.7 indices given by NASA Goddard Space Flight Center, the date of disturb and calm ionosphere is preliminarily selected (http://omniweb.gsfc.nasa.gov/form/dx1.htm1). The date of calm ionosphere activity is 2017day315 UT 00:00:00–23:59:59, and the date of disturb ionosphere activity is 2003day302 UT 00:00:00–23:59:59. The corresponding indices of the two days are shown in Fig. 1.
- Furthermore, we confirm the ionosphere activity status of a specific region by comparing the spatial variation gradient [14] of vTEC near the station on different dates. We take the geomagnetic low latitude BOGT station in Table 1 as an example. (It is generally considered that the ionosphere characteristics are more complex in the geomagnetic low latitudes, so we chose the BOGT station here, and the results of other stations are similar). Using the precise ephemeris and observation files broadcast by IGS and the satellite and station DCB products from CODE IONEX file, we may obtain the local vTEC results. The vTEC results in the region near the BOGT station under 2003day302 and 2017day315 are shown in Fig. 2(a) and Fig. 2(b) respectively.

The horizontal axis represents the longitude, the vertical axis represents the latitude, and both of the units are degrees. In Fig. 2, the contours are used to represent the vTEC results at different locations, and the values on the contours represent the vTEC results in TECU. By comparing the relationship between the change of vTEC value and the change of distance between the contours, we can qualitatively obtain the gradient of vTEC in different positions and directions. By comparing the (a) and (b), it can be seen that the vTEC gradient under 2003day302 is much larger than that under 2017day315. Therefore, we can regard that the ionosphere under the 2003day302 is more active.

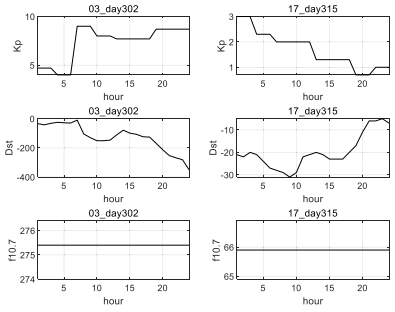

Fig. 1 The K_p, D_{st} and f10.7 indices under the date of disturb (2003day302) and calm (2017day315) ionosphere.

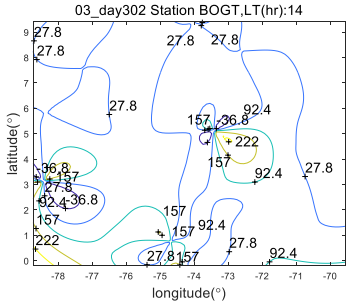

(a) disturb (2003day302)

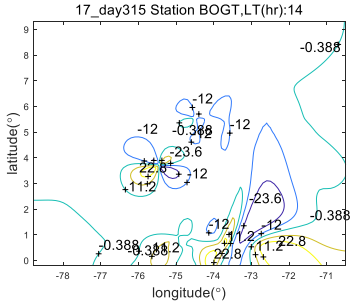

(b) calm (2017day315)

Fig. 2 The spatial variation gradient of vTEC near the BOGT station on different dates.

3.1.2 The Local Ionosphere Characteristics under Different Ionosphere Status

We have confirmed the ionosphere activity state of the selected date. Below, we will intuitively show the vTEC modeling performance of the constant model and the linear planar model under different ionosphere states. Figure 3 shows the vTEC modeling results for UT 2003dy302:18:55:00 and UT 2017day315 18:55:00 at BOGT station, corresponding to the local time LT 2003day302 14:00:00 and LT 2017day315 14:00:00, respectively.

In Fig. 3, the x axis and y axis represent latitude and longitude, respectively, in units of degree. The z axis represents vTEC results in TECU (TEC Unit, 1 TECU=10^{16}/m^2). The blue dots represent the measured vTEC results of the IPPs from the dual-frequency observations of IGS station, and the black and red dots represent the estimation results of the IPPs' vTEC by using the constant model and the first-

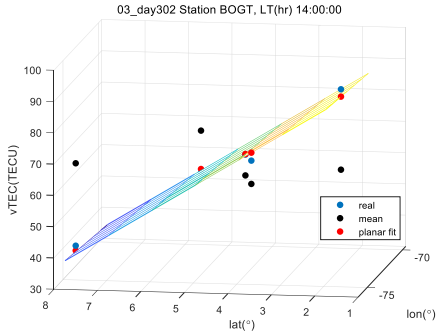

(a) disturb (2003day302)

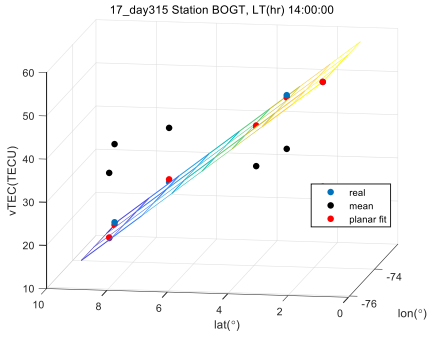

(b) calm (2017day315)

Fig. 3 The vTEC modeling results of the two models under disturb and calm ionospheric status for BOGT station.

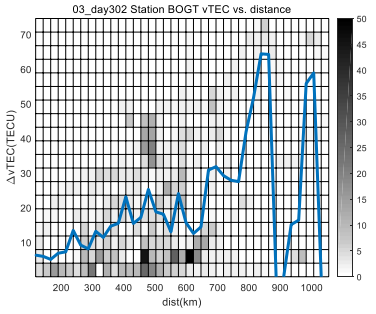

(a) disturb (2003day302)

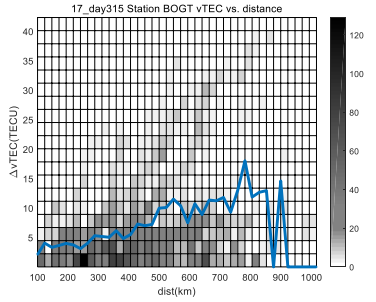

(b) calm (2017day315)

Fig. 4 The relationship between IPP GCD and Δ vTEC under different ionosphere status for BOGT station.

order linear planar model, respectively. It can be seen that the linear planar model can achieve better modeling performance with smaller bias to the measured data.

We have already demonstrated the ionospheric characters at a time instant. Next, we will show its statistical property over a longer period. The relationships between the *vTEC* difference of IPP pairs and their great circle distances are shown in Fig. 4(a) and Fig. 4(b), which represent the results in disturb and calm ionosphere status respectively.

The horizontal axis represents the distance in kilometers, and the vertical axis represents the vTEC difference ($\Delta vTEC$) between the two IPPs (in the unit of nanoseconds). Different grayscale is used to distinguish the occurrence frequency of events fall within the grid. To quantify the results, we introduce the indicator of Avg_j, which is the average of $\Delta vTEC$ within a certain IPP distance grid (the blue lines in Fig. 4). It can be expressed as,

$$Avg_j = \frac{1}{N_j} \sum_{i=1}^{N_{bin}} \Delta vTEC_i n_{i,j} \tag{10}$$

where j stands for a certain IPP distance interval, N_{bin} is the total number of $\Delta vTEC$ bins in vertical axis, $n_{i,j}$ denotes the number of incidents whose IPP distances and $\Delta vTEC$s fall in the specific bin. N_j is the total number of events in the jth IPP distance interval, and we have that,

$$N_j = \sum_{i=1}^{N_{bin}} n_{i,j} \tag{11}$$

From the above two figures we can see the linear planar trend of vTEC in a local scale (or when the distance is small), and the linear planar model is more in line with the actual ionosphere characteristics than the constant model. In this paper, we model the vTECs as [15],

$$vTEC^i_j = a_0 + a_1 lon^i_j + a_2 lat^i_j \tag{12}$$

where lat^i_j and lon^i_j represent the latitude and longitude coordinates of IPPs, a_0, a_1 and a_2 are the coefficients of the zero-order terms and the two first-order terms in the longitude and latitude directions, respectively.

3.2 Minimum STD Searching Algorithm Based on Linear Planar Model

Based on the vTEC model mentioned before, we theoretical validate the correctness of our planar fit method.

To simplify the expression, we take a substitution in Eq. (6), where $x^i_j = vTEC^i_j$, $k^i_j = \left(\frac{A(f_1^2 - f_2^2)}{c f_1^2 f_2^2} \frac{1}{E(\Theta^i_j)}\right)^{-1}$, $y^i_j = \tilde{L}^i_j(t) - D^i$. The subscript j which stands for different receivers is omitted because we study the single station DCB estimation problem here. Equation (6) can be expressed as,

$$x^i + k^i D = k^i y^i \tag{13}$$

Suppose D and $\tilde{D}$ are the true and estimated value of receiver DCB. Their relationship is,

$$\tilde{D} = D + \Delta D \tag{14}$$

Like that in Eq. (9), the objective function can be expressed

as,

$$J = \frac{1}{N}\sum_{t=1}^{N}\frac{1}{M_t}\sum_{i=1}^{M_t}\left(x^i(t) - \tilde{x}^i(t)\right)^2 \tag{15}$$

where $\tilde{x}^i(t)$ is the estimation for $x^i(t)$ of the time epoch t. The objective function reaches its minimum when the STD estimations under all epochs are in their minimum. We first have a research on the J_t of a single epoch and show the conditions for an unbiased estimation. Then we will explain that all the conditions for all time epochs could be satisfied simultaneously.

Take ΔD as the independent variable, we substitute Eqs. (12) and (14) into Eq. (15), the objective function for a single epoch is (where the subscript t is omitted for simplicity),

$$J_t(\Delta D) = \frac{1}{M_t}\sum_{i=1}^{M_t}\left[x^i + k^i\Delta D - \left(\tilde{a}_0 + \tilde{a}_1 lon^i + \tilde{a}_2 lat^i\right)\right]^2 \tag{16}$$

$\tilde{a}_0$, $\tilde{a}_1$ and $\tilde{a}_2$ are the least square results corresponding to Eq. (12).

$$\tilde{a} = \begin{bmatrix}\tilde{a}_0 & \tilde{a}_1 & \tilde{a}_2\end{bmatrix}^T = \left(H^T H\right)^{-1} H^T X \tag{17}$$

Where,

$$H = \begin{bmatrix} 1 & lon^1 & lat^1 \\ 1 & lon^2 & lat^2 \\ \cdots & \cdots & \cdots \\ 1 & lon^{M_t} & lat^{M_t} \end{bmatrix} \tag{18}$$

$$\begin{aligned} X &= \begin{bmatrix} y^1 - k^1\tilde{D} & \cdots & y^{M_t} - k^{M_t}\tilde{D}\end{bmatrix}^T \\ &= \begin{bmatrix} x^1 + k^1\Delta D & \cdots & x^{M_t} + k^{M_t}\Delta D\end{bmatrix}^T \end{aligned} \tag{19}$$

The solutions in Eq. (17) are the unbiased estimation if we suggest that the observation noise is Gaussian. Therefore, the $\tilde{x}^i(t)$ is also unbiased for it is a linear combination of $\tilde{a}$. Substituting Eq. (17) into Eq. (16), we could have that,

$$\begin{aligned} J_t(\Delta D) = \frac{1}{M_t}\sum_{i=1}^{M_t}\Bigg[&\begin{bmatrix}0 & \cdots & \underset{i}{1} & \cdots & 0\end{bmatrix}\begin{bmatrix} x^1 + k^1\Delta D \\ \cdots \\ x^i + k^i\Delta D \\ \cdots \\ x^{M_t} + k^{M_t}\Delta D\end{bmatrix} \\ &- \begin{bmatrix}1 & lon^i & lat^i\end{bmatrix}\left(H^T H\right)^{-1} H^T \begin{bmatrix} x^1 + k^1\Delta D \\ \cdots \\ x^i + k^i\Delta D \\ \cdots \\ x^{M_t} + k^{M_t}\Delta D\end{bmatrix}\Bigg]^2 \end{aligned} \tag{20}$$

Take that,

$$W_i = \begin{bmatrix}0 & \cdots & \underset{i}{1} & \cdots & 0\end{bmatrix} - \begin{bmatrix}1 & lon^i & lat^i\end{bmatrix}\left(H^T H\right)^{-1} H^T \tag{21}$$

$$K = \begin{bmatrix}k^1 & k^2 & \cdots & k^{M_t}\end{bmatrix}^T \tag{22}$$

The $J_t(D)$ can be expressed as,

$$J_t(\Delta D) = \frac{1}{M_t}\sum_{i=1}^{M_t}\left[W_i(X + K\Delta D)\right]^2 \tag{23}$$

Making the partial derivation of , we may get that,

$$\frac{\partial J_t(\Delta D)}{\partial \Delta D} = \frac{2}{M_t}\sum_{i=1}^{M_t}(W_i X W_i K + \Delta D W_i K W_i K) = dJ_1 + dJ_2 \tag{24}$$

$$dJ_1 = \frac{2}{M_t}\sum_{i=1}^{M_t} W_i X W_i K \tag{25}$$

$$dJ_2 = \frac{2}{M_t}\sum_{i=1}^{M_t}\Delta D W_i K W_i K \tag{26}$$

And,

$$\begin{aligned} W_i X = \Bigg(&\begin{bmatrix}0 & \cdots & \underset{i}{1} & \cdots & 0\end{bmatrix} \\ &- \begin{bmatrix}1 & lon^i & lat^i\end{bmatrix}\left(H^T H\right)^{-1} H^T\Bigg) X = x^i - \tilde{x}^i \end{aligned} \tag{27}$$

Because of the unbiased nature of x^i, the difference between x^i and $\tilde{x}^i$ can be regarded as noise, the first term dJ_1 on the right hand of Eq. (24) is zero. Thus we may have the conclusion that when $\Delta D = 0$, the objective function (namely the sum of STDs) J_t reaches its minimum. And with the growth of the absolute value of ΔD, the J_t will also increase. For the reason that the matrix W is obtained by the observations of the corresponding time epoch, which is independent from the others, the conditions for unbiased estimation can be satisfied simultaneously.

Further, by analyzing Eq. (25) and Eq. (27), we could also found the problems in traditional constant model based minimum STD searching method. For the reason that the constant value of vTECs cannot be treated as unbiased estimations, the result of dJ_1 will no longer be zero. Thus, in order to minimize the objective function, namely to set the partial derivation of $J_t(D)$ to be zero, the ΔD must not be zero. Then we may conclude that the receiver DCB estimated from minimization STD will have bias when inappropriate estimated vTECs are being used.

3.3 Estimation Bias Detection

The traditional method sums all the vTEC standard variances from different epochs together and takes the value which makes a minimum as the receiver DCB estimation result. As proposed before, the key for the establishment of the algorithm is the degree of agreement between the planar fit model and the actual ionosphere characteristics, namely the relationship between dJ_1/dJ_2 which generated from Eq. (25) and Eq. (26) and zero. Thus we design a estimation bias detector dJ,

$$dJ = dJ_1/dJ_2 \tag{28}$$

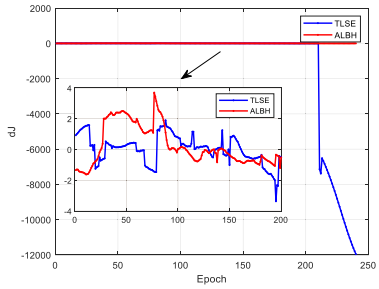

Fig. 5 The dJ results when different estimation biases are considered.

Table 2 The disturb data set used for dJ threshold design.

date	K_p	D_{st}
10/29/2003 (day302)	9.0	-350
10/30/2003 (day303)	9.0	-383
10/31/2003 (day304)	8.3	-387
11/20/2003 (day324)	8.7	-422
11/21/2003 (day325)	6.7	-309
07/17/2004 (day199)	6.0	-76
11/08/2004 (day313)	8.7	-374
11/09/2004 (day314)	8.7	-214
11/10/2004 (day315)	8.7	-263

dJ is the ΔD in Eq. (24) actually.

Figure 5 shows the dJ results when different estimation biases are considered. We take the data from 2003/10/29 as examples. For small estimation bias, we use the result from station ALBH (48.39°N, 123.49°W), whose reference DCB is 7.182 ns from the CODE IONEX file and estimated DCB is 6.822 ns using the algorithm proposed in Sect. 3.2. For large estimation bias, we use the result from station TLSE (43.56°N, 1.48°E), whose reference DCB is 0.882 ns and estimated DCB is 10.882 ns. As the searching interval set in this paper is 10 ns, the algorithm can be regarded as invalid under this situation.

It can be seen that both the amplitude of dJ and the occurrence frequency of large dJ increase greatly when large estimation bias exists. If we still use the vTEC variances from all the epochs to find the DCB value, the estimation result may have a severe derivation, especially in disturbed ionospheric status. Considering the receiver DCB is a slowly changing quantity and thus can be regarded as a constant during the analysis periods (one day in this paper), the data can be selected to have a better result. We can settle a dJ threshold and only the data whose dJ value is smaller than the threshold can be used to estimate DCB result. We statistically analyze the relationship between the DCB estimation bias and the dJ value, and find the preliminary threshold. Because the purpose of threshold is to avoid the existence of large biases which often occur during disturbed ionosphere conditions, we use data (in disturb ionosphere status) listed below to accomplish our analysis.

The relationship is shown in Fig. 6. The color bar stands for the number of events that fall within the grid. Lines in blue represent the mean value of the DCB estimation biases under different dJ values. (Events are concentrated in the grids with smaller dJ values. The tail part of the figures have violently fluctuates because of the lack of samples). The linear trend can be seen clearly, and the DCB estimation bias increases as the dJ value increase. In this paper, we choose $dJ = 5$ as the threshold.

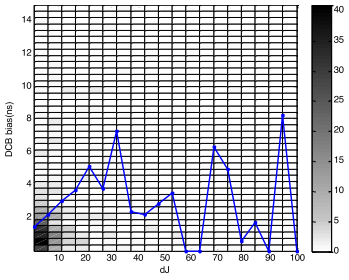

Fig. 6 The relationship between the DCB estimation bias and the dJ value.

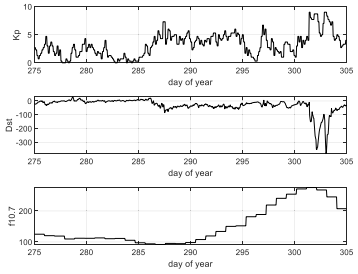

Fig. 7 The ionosphere activity indices (K_p, D_{st} and f10.7) from 2003day270 to 2003day305.

4. Experimental Results

This section analyzes the performance of the linear planar based minimum STD searching algorithm under different seasons, different geomagnetic latitudes and different ionosphere status. Also the results are compared with that of the traditional algorithm which based on constant model. Comparisons show the correctness and effectiveness of the proposed method.

4.1 Performance under Different Geomagnetic Latitudes

We select 2003day270–2003day305 as the analysis period, and take the three stations with different geomagnetic latitudes listed in Table 1 as the objects, to compare the differences of the DCB estimation results between the constant model based and the linear planar model based approach. The influence of the geomagnetic latitude to the performance of the algorithm is explained.

We first show the ionosphere activity indices (K_p, D_{st} and f10.7) from 2003day270 to 2003day305.

It can be seen from the figure that the ionosphere state changed from calm to disturb during this period of time. During the 2003day270 to 2003day285, the ionosphere can be regarded in a calm state, where the K_p values are less than 5 and the D_{st} values are greater than -10. After 2003day285, the ionosphere became active, between 2003day300 to 2003day305, there was a severe geomag-

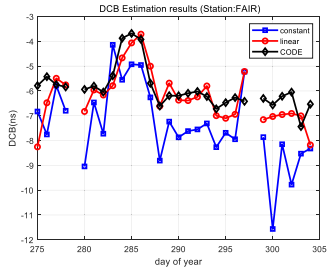

(a) FAIR

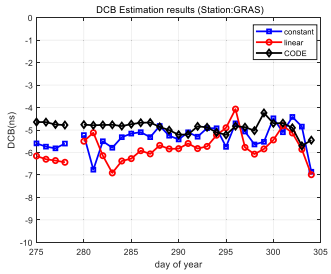

(b) GRAS

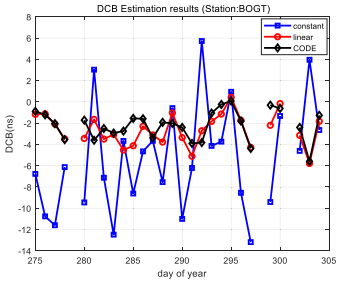

(c) BOGT

Fig. 8 The DCB estimation results of FAIR, GRAS and BOGT stations during the above analysis period.

Table 3 The standard deviations of the DCB estimation results of three stations from 2003day270 to 2003day305 (in ns).

Method	FAIR	GRAS	BOGT
Constant	1.59	0.55	5.02
Linear Planar	1.07	0.62	1.49
CODE	0.84	0.28	1.38

netic storm causing major disturbance in the ionosphere.

Figure 8(a), (b) and (c) give the DCB estimation results of FAIR, GRAS and BOGT stations (located in geomagnetic high, mid and low latitude respectively) during the above analysis period.

In Fig. 8, the horizontal axis represents the date, and the vertical axis represents the DCB results in nanosecond. The blue curve represents the estimation result of the traditional method, the red curve represents the estimation result obtained by the proposed method, and the black curve is the CODE result, which is used as reference here. Table 3 below shows the standard deviations of the DCB results of three stations during the analysis period.

From Fig. 8 and Table 3, it can be seen that compared with the traditional constant model based minimum STD searching algorithm, the standard deviation of the estimated DCBs which obtained by our proposed method is smaller

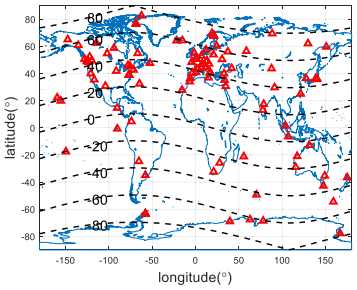

Fig. 9 The Distribution of selected stations.

and the DCB values are closer to the CODE product. For the geomagnetic high and mid latitude, the STDs of the DCB estimation under the two methods are both smaller than 2ns. However, for BOGT stations at low geomagnetic latitudes, the STD of the DCB estimation under the constant model based approach is about 5 ns, which is much larger than that of the linear planar based approach. Under the traditional method, the geomagnetic latitudes have stronger influence on DCB estimation performance, especially in the low geomagnetic latitudes. While our proposed method can effectively alleviate this kind of influence.

4.2 Performance under Different Seasons

In this subsection, we take 2018/02/14 (spring), 2018/05/15 (summer), 2017/08/13 (autumn) and 2017/11/11 (winter) as examples to analyze the DCB estimation performance under different seasons. We randomly select 100 IGS stations for algorithm verification. The distribution of the station is shown in Fig. 9.

In Fig. 9, the horizontal and vertical axis represents the geographic longitude and latitude, respectively. The longitude range is from $-180°$ to $180°$, and the positive and negative values correspond to the eastern and western longitude. The latitude range is from $-90°$ to $90°$, and the positive and negative values correspond to the northern and southern latitude. The red triangle represents station location. The black dotted lines represent the geomagnetic latitudes, and the number on the line represents the geomagnetic latitude value.

Figure 10 shows the difference between the DCB estimation results and the CODE results. The blue squares represent the result under the constant model based approach, and the red circles represent the result under the linear planar model based approach. The horizontal axis represents the geomagnetic latitudes corresponding to different stations and in the unit of degree. The vertical axis represents the difference between the DCB estimation results and the CODE products and in the unit of ns.

If we take the products given by CODE as the “truth”, the difference between the estimated result and the “truth” can be treated as the evaluation criterion for the performance of the algorithm. In fact, this has a similar meaning to the variance analysis of DCB estimations in the usual sense. Because the products of CODE can be considered to be the

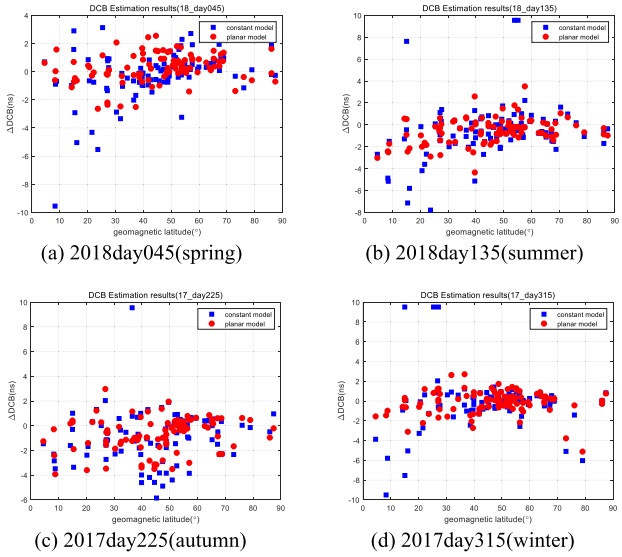

(a) 2018day045(spring) (b) 2018day135(summer)

(c) 2017day225(autumn) (d) 2017day315(winter)

Fig. 10 The difference between the DCB estimation results and the CODE results under different seasons.

Table 4 The average deviation between the calculated DCB results and the CODE results at high, mid and low geomagnetic latitudes under different seasons (in ns).

		2018day045 (spring)	2018day135 (summer)	2017day225 (autumn)	2017day315 (winter)
High	I	0.75	0.92	0.81	1.05
	II	0.77	0.68	0.78	0.88
Mid	I	0.99	1.33	1.67	1.00
	II	0.81	0.93	1.21	0.85
Low	I	1.42	2.06	2.05	2.28
	II	2.80	1.81	1.33	1.09
All	I	1.31	1.50	1.56	1.37
	II	0.79	0.97	1.15	0.88

most accurate estimation of the real DCB at the current technical level, thus the closer it is to the CODE result, the more accurate can be considered. It can be seen from Fig. 10 that there is no obvious seasonal difference in the DCB estimation results of the two methods during the relative calm period of the ionosphere. However, compared with the traditional constant model based method, the proposed method can effectively alleviate the occurrence of large estimation errors (compared with CODE results).

Furthermore, we statistically analysis the results shown in Fig. 10 and give the quantitative results in Table 4. The rows in Table 4 represent different dates, and the columns represent the average deviation between the calculated DCB results and the CODE results at high, mid and low geomagnetic latitudes (the deviations are in their absolute values). The results are in the unit of nanosecond.

In Table 4, "I" and "II" represent the constant model based and linear planar model based minimum STD searching algorithm, respectively. The "High", "Mid", and "Low" represent the geomagnetic latitude. The "All" in the last row represents the results of all stations. It can be seen that there is no obvious seasonal difference of the two algorithms during the quiet period of the ionosphere. The average deviation of DCB estimation results under the traditional constant

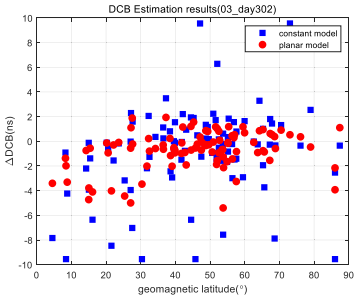

Fig. 11 The difference between the DCB estimation results and the CODE results under disturb ionosphere status.

model and the proposed linear planar model is about 1.3ns and 1ns compared with the CODE results. The DCB estimated by the linear planar model based approach is closer to the CODE results, also the maximum estimation deviation is much smaller. For the two DCB estimation algorithms, the average deviation of DCB estimation in geomagnetic low latitude stations is slightly larger than that of geomagnetic high and mid latitudes, which is related to the more complex ionosphere activity in the low latitudes.

4.3 Performance under Different Ionosphere Status

Under the station distribution given in Fig. 9, we analyze the DCB estimation performance of the two algorithms under the condition of disturb ionosphere. We take 2003day302 as an example to give the results. The horizontal and vertical axis and the markers in the Fig. 11 have the same meaning as in Fig. 10.

It can be seen that during the disturb ionosphere status, the DCB estimation results obtained by the traditional minimum variance search method have a large deviation compared with the CODE results. However, our proposed algorithm which can better model the vTEC characteristics of the local ionosphere and complete the selection of epochs with the help of bias detection indicator dJ, may have a better DCB estimation performance. Results show that the maximum deviation may reach the setting boundary (9.55 ns) for the traditional method, the deviation at 90% quartile is 7.03 ns, and the average deviation is 2.30 ns. The maximum deviation for our proposed method is 5.40 ns, the deviation at 90% quartile is 3.31 ns, and the average deviation is 1.22 ns, which are all smaller than that of the traditional method. It means that the results calculated from our proposed method are closer to the CODE result. Further, we statistically analysis the DCB estimates for 2003/10/29, 2003/10/30, 2003/10/31, 2003/11/20 and 2003/11/21 in Table 5 (the K_p and D_{st} indicators for these five days are shown in Table 2). In Table 5, we also classify the stations according to their geomagnetic latitudes.

The meaning of "I" and "II" are the same as what in Table 4. It can be seen that the average deviation between the DCB estimated by the linear planar model based minimum STD searching algorithm and the results given by CODE is about 1ns, while that is about 2 ns for the tradi-

Table 5 The average deviation between the calculated DCB results and the CODE results under disturb ionosphere status (in ns).

		2003day302	2003day303	2003day304	2003day324	2003day325
High	I	2.67	1.94	2.68	1.05	1.34
	II	0.98	0.90	0.81	0.54	0.84
Mid	I	2.01	2.58	2.36	1.67	2.38
	II	1.12	1.29	1.24	0.98	1.03
Low	I	4.06	6.07	4.82	5.79	3.22
	II	2.67	2.33	3.23	2.82	2.25
All	I	2.30	2.79	2.66	1.91	2.25
	II	1.22	1.32	1.35	1.06	1.11

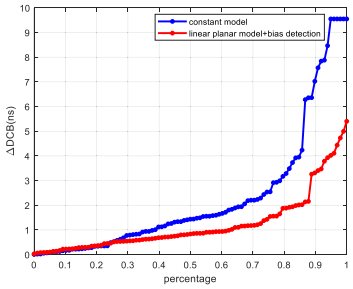

Fig. 12 The empirical distribution of DCB estimation derivations of the two algorithms under the disturb ionosphere days.

tional one. That is, the results obtained by the proposed method are closer to those given by CODE. In addition, by comparing with the results in Table 4 which represents the calm ionosphere status, it can be found that the average deviation increases under the disturb ionosphere status, which indicates that the consistency between the model assumptions and the ionosphere characteristics is also an important factor affecting the performance of the algorithm. For stations with different geomagnetic latitudes, the DCB estimation performance is also different, and the results in low latitudes is worse than that in mid and high latitudes, which is consistent with the analysis results in Sects. 4.1 and 4.2. Figure 12 below calculates the empirical distribution of DCB estimation derivations of the two algorithms under the disturb ionosphere days.

In Fig. 12, the horizontal axis stands for the percentage, and the vertical axis represent the difference between the estimated DCB results and the CODE results. The blue curve represents the distribution of DCB estimation deviations which are obtained from the constant model based algorithm, and the red curve represents the one generated from the linear planar model based approach with the dJ bias detection. It can clearly see that from the traditional method is much more likely to produce a large estimation deviation in the case of disturb ionosphere status, but the method proposed in this paper can still effectively control the amplitude of the maximum deviation in this situation.

5. Conclusions

In this paper, we first summarize the existing single station DCB estimation methods with emphasis on the principle and hypothesis of the minimum STD searching algorithm. Secondly, based on the analysis of ionosphere vTEC data, a linear planar model is introduced to describe the characteristics of the local ionosphere. And the advantages of the proposed linear planar model based algorithm are proved by theoretical analysis. Finally, the performance of the proposed algorithm in different geomagnetic latitudes, different seasons and different ionosphere states is analyzed and compared with the traditional constant model based algorithm to show its effectiveness.

The experimental results show that there is no obvious performance difference between different seasons. For the traditional minimum STD searching algorithm based on constant model, latitude difference is the key factor affecting the performance of DCB estimation. The DCB estimation performance in geomagnetic mid latitudes is the best, followed by the high latitudes and the worst is for the low latitudes. This phenomenon is consistent with the complex characteristics of ionosphere activity in the low geomagnetic latitudes. The algorithm proposed in this paper can effectively solve the performance degradation problem of DCB estimation in geomagnetic low latitudes by using the linear planar model which is with a higher degree of freedom to model the local ionosphere characteristics and design dJ to screen the epochs. Through the analysis of the DCB estimation results of a large number of stations, it can be found that the probability of large estimation deviation of the traditional method will increase obviously under the disturb ionosphere conditions, but the algorithm we proposed can effectively control the amplitude of the maximum deviation and alleviate the probability of large estimation deviation in disturb ionosphere status.

Acknowledgments

This work is supported by National Natural Science Foundation of China (No. 61601485).

References

[1] G.E. Lanyi and T. Roth, "A comparison of mapped and measured total ionospheric electron content using global positioning system and beacon satellite observations," Radio Sci., vol.23, no.4, pp.483–492, 1988.

[2] D.S. Coco, C. Coker, S.R. Dahlke, and J.R. Clynch, "Variability of GPS satellite differential group delay biases," IEEE Trans. Aerosp. Electron. Syst., vol.27, no.6, pp.931–938, 1991.

[3] S. Schaer, Mapping and Predicting the Earth's Ionosphere using Global Positioning System, Doctoral Dissertation, Astronomy Institute, University Bern, Switzerland, 1999.

[4] E. Sardón, A. Rius, and N. Zarraoa, "Estimation of the transmitter and receiver differential biases and the ionospheric total electron content from global positioning system observations," Radio Sci., vol.29, no.3, pp.577–586, 1994.

[5] Y. Yuan and J. Ou, "A generalized trigonometric series function model for determining ionospheric delay," Prog. Nat. Sci., vol.14, no.11, pp.1010–1014, 2004.

[6] J. Liu, Z. Wang, H. Zhang, and W. Zhu, "Comparison and consistency research of regional ionospheric TEC models based on GPS measurements," Geomatics and Information Science of Wuhan University, vol.33, no.5, pp.479–483, 2008.

[7] Y. Otsuka, T. Ogawa, A. Saito, T. Tsugawa, S. Fukao, and S. Miyazaki, "A new technique for mapping of total electron content

using GPS network in Japan," Earth Planet Sp, vol.54, pp.63–70 2002.
[8] F. Arikan, H. Nayir, U. Sezen, and O. Arikan, "Estimation of single station interfrequency receiver bias using GPS-TEC," Radio Sci., vol.43, no.4, RS4004, 2008.
[9] G. Ma and T. Maruyama, "Derivation of TEC and estimation of instrumental biases from GEONET in Japan," Ann. Geophys, vol.21, no.10, pp.2083–2093, 2003.
[10] R. Jin and S. Jin, "M_DCB: Matlab code for estimating GNSS satellite and receiver differential code biases," GPS Solutions, vol.16, no.4, pp.541–548, 2012.
[11] X. Ren, X. Zhang, W. Xie, K. Zhang, Y. Yuan, and X. Li, "Global ionospheric modelling using multi-GNSS: BeiDou, Galileo, GLONASS and GPS," Sci. Rep., vol.6, 33499, 2016.
[12] J. Xue, S. Song, and W. Zhu, "Estimation of differential code biases for Beidou navigation system using multi-GNSS observations: How stable are the differential satellite and receiver code biases?," J. Geodesy, vol.90, no.4, pp.309–321, 2016.
[13] C.C. Finlay, S. Maus, C.D. Beggan, M. Hamoudi, F.J. Lowes, N. Olsen, and E. Thébault, "Evaluation of candidate geomagnetic field models for IGRF-11," Earth Planet Sp, vol.62, 8, 2010, https://doi.org/10.5047/eps.2010.11.005
[14] T. Dugassa, J.B. Habarulema, and M. Nigussie, "Spatial gradient of total electron content (TEC) between two nearby stations as indicator of occurrence of ionospheric irregularity," Annales Geophysicae Discussions, pp.1–19, 10.5194/angeo-2018-131, 2018.
[15] J. Blanch, Using Kriging to Bound Satellite Ranging Errors due to the Ionosphere, Doctoral Dissertation, The Department of Aeronautics and Astronautics, Stanford University, USA, 2004.

Yan Zhang received the B.S. degree and M.S. degree in information and communication engineering from National University of Defense Technology. She is now a Ph.D. candidate majoring in SBAS integrity. She is now worked in Satellite Navigation R&D Center of National University of Defense Technology.

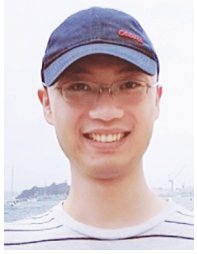

Lei Chen is a lecturer, majors in signal acquisition and tracking, hardware design, FPGA coding in Global Navigation Satellite System. He has worked in Satellite Navigation R&D Center of National University of Defense Technology since 2010. He received a M.S. and a Ph.D. from College of Electronic Science, National University of Defense Technology.

Xiaomei Tang is a lecturer, majors in weak signal acquisition and tracking, long code acquisition in Global Navigation Satellite System. She has worked in Satellite Navigation R&D Center of National University of Defense Technology since 2003. She received a M.S. and a Ph.D. from College of Electronic Science, National University of Defense Technology.

Gang Ou is a professor, majoring in Global Navigation Satellite System signal processing. He received the M.S. and Ph.D. degrees from College of Electronic Science, National University of Defense Technology.